Shear creep behaviour of soil-structure interfaces under thermal cyclic loading

Golchin, A.; Guo, Y.; Vardon, P. J.; Liu, S.; Zhang, G.; Hicks, M. A.

Important note
To cite this publication, please use the final published version (if applicable).
Please check the document version above.

Shear creep behaviour of soil–structure interfaces under thermal cyclic loading

A. GOLCHIN†, Y. GUO*†, P. J. VARDON‡, S. LIU*, G. ZHANG* and M. A. HICKS†

The coupling effect of initial shear stress and thermal cycles on the thermomechanical behaviour of clay concrete and sand–concrete interfaces has been studied. A set of drained monotonic direct shear tests was conducted at the soil–concrete interface level. Samples were initially sheared to half of the material's shear strength and then they were subjected to five heating/cooling cycles before being sheared to failure. The test results showed that the effect of thermal cycles on the shear strength of the materials was negligible, yet shear displacement occurred during application of thermal cycles without an increase in shear stress, confirming the coupling between the shear stress and temperature. In addition, a slight increase of stiffness due to the coupling was observed which diminished with further shearing.

INTRODUCTION

The application of thermo-active geo-structures such as energy piles and thermal diaphragm walls (Makasis & Narsilio, 2020) has gained attention in the past decade for extracting energy and heat from shallow geothermal resources (mostly soil layers), due to their low cost and reasonable long-term sustainability (Brandl, 2006). Such geo-structures are designed to bear mechanical loads (as their main purpose) by transferring the loads to the ground, and to exchange heat with the surrounding soil. Due to thermal effects on the mechanical behaviour of the structure and the surrounding soil, as well as their coupling effects, thermo-active geo-structures have a more complex soil–structure interaction compared to regular geo-structures that do not exchange heat. Therefore, such structures are exposed to a number of extra potential loads that must be considered in the design procedure, such as additional settlements which may negatively affect the serviceability of the system and a reduction in bearing capacity which may negatively affect the system's stability.

Prior to being exposed to temperature changes, soil elements adjacent to thermo-active geo-structures experience a wide range of shear stresses and shear strains, due to the installation procedure and carrying mechanical loads. In addition, soil elements at the interface level are subjected to daily and seasonal thermal cycles. Therefore, it is essential to investigate the effects of thermal cycles on the thermomechanical behaviour of soil–structure interfaces with pre-existing shear stresses and strains. Several investigations have been carried out to study the effect of thermal cycles on the

behaviour of soil–structure interfaces (Di Donna *et al.*, 2016; Yavari *et al.*, 2016; Li *et al.*, 2019; Vasilescu *et al.*, 2019; Yazdani *et al.*, 2019; Maghsoodi *et al.*, 2020; Ravera *et al.*, 2021; Guo *et al.*, 2023). In general, thermal cycles were found to have a limited effect on the soil–interface strength and deformation. However, previous studies mostly considered the effect of thermal cycles without shear stresses being applied. In energy geo-structures, due to the structural loads, interfaces are likely to be subjected to mechanical (shear) loads prior to application of the thermal loads. In this paper, the coupling effects of thermal cycles with constant shear stresses on the behaviour of soil–structure interfaces are investigated, which is one of the first studies investigating this phenomenon.

Direct shear element tests have been used here as they resemble the mechanism of shear strength mobilisation at the interface layer between soil and structures (Boulon & Foray, 1986) and may mimic many boundary conditions (BCs) that are applied on interface layers, affecting the mechanical behaviour of the interface layer. During shear deformation, volumetric deformation may occur which may change the normal stresses acting on the layer. In direct shear tests, three scenarios are often used for the BCs and these may be quantified by the normal stiffness (K) acting on the interface layer, which is the ratio of the rate of normal stress ($\Delta\sigma_n$) applied on the interface layer and the rate of measured normal displacement ($\Delta\delta$) (i.e. $K = \Delta\sigma_n/\Delta\delta$). The BCs may be mimicked as springs with a stiffness of K (Fakharian & Evgin, 1997) attached to the soil (Fig. 1). Assuming a zero stiffness for the springs (i.e. $K = 0$), conventional direct shear tests known as constant normal load (CNL) may be performed (Fig. 1(a)). By keeping the K value constant during shearing, it is possible to perform a constant normal stiffness (CNS) test by way of a direct shear apparatus (Fig. 1(b)). This may be most representative of field conditions, although it has challenges in determining the appropriate stiffness because it is typically problem and material dependent. On the contrary, an infinite normal stiffness results in a constant volume (CV) shear test which can represent undrained conditions (Fig. 1(c)).

In this study, as the most significant temperature cycles in thermo-active geo-structures are annual and the aim is to illustrate fundamental material behaviour, rather

*Institute of Geotechnical Engineering, Southeast University, Nanjing, Jiangsu, P. R. China.
†Section of Geo-engineering, Faculty of Civil Engineering and Geosciences, Delft University of Technology, Delft, the Netherlands.
‡Section of Geo-engineering, Faculty of Civil Engineering and Geosciences, Delft University of Technology, Delft, the Netherlands (Orcid:0000-0001-5614-6592).
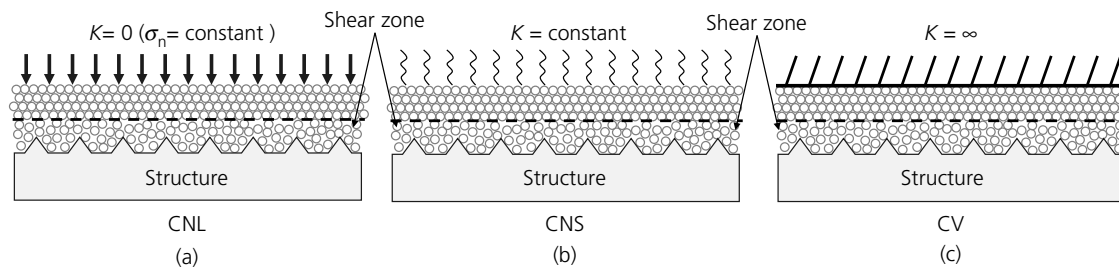
Fig. 1. Schematic of BCs normal to the soil interface: (a) CNL; (b) CNS; (c) CV

than a problem-specific behaviour, CNL conditions are selected.

EXPERIMENTAL SET-UP AND MATERIALS

A detailed description of the experimental set-up and materials used in this study are provided in Part A and in Part B of the online Supplementary Material, respectively. Here, only a brief summary is given.

The thermomechanical interface behaviour between a concrete block and a fine uniform silica sand (commercially known as Geba sand), and Speswhite clay consisting of kaolinite and illite, was investigated by direct shear tests using CNL conditions. CNL conditions were selected as these represent the fundamental soil behaviour, which is most easily translated into constitutive models (which can include more complex stress paths). In addition, it would be representative of field conditions of energy piles under long-term monotonic loading conditions where shear creep occurs under almost constant normal stress. Medium dense (relative density, $D_r = 50\%$) sand samples with a thickness of 20 mm were prepared by uniformly pouring dry sand into a shear box and compacting using a tamping method to reach a dry density of 1.43 g/cm^3, and then fully saturating. Homogenous kaolin slurry with a water content of 1.5 times the liquid limit was first consolidated using a large oedometer cell and then trimmed using a cutting ring.

A $10 \times 10 \times 1$ cm concrete block was placed in the lower compartment of a temperature-controlled direct shear apparatus. The apparatus was placed in a climate room at a constant temperature of 20°C. Embedded heat exchangers in the thermally insulated load cap and the base of carriage, which were connected to a heat pump, facilitated the temperature variation in the soil sample and concrete block. The temperature at the interface was measured by way of a PT100 sensor placed in a pre-drilled hole in the concrete block.

The vertical and horizontal displacements were measured by way of two linear variable differential transformers (LVDTs) with a resolution of 0.001 mm. In soil element tests, temperature changes may exert an influence on the displacement and force readings due to thermal expansion/contraction of the apparatus and equipment temperature shift. Here, these effects were considered by calibrating the LVDTs and force measurements by mimicking the thermo-mechanical tests on a dummy iron sample, following the same thermo-mechanical paths as in the experimental programme (see Part A of the online Supplementary Material for a detailed explanation).
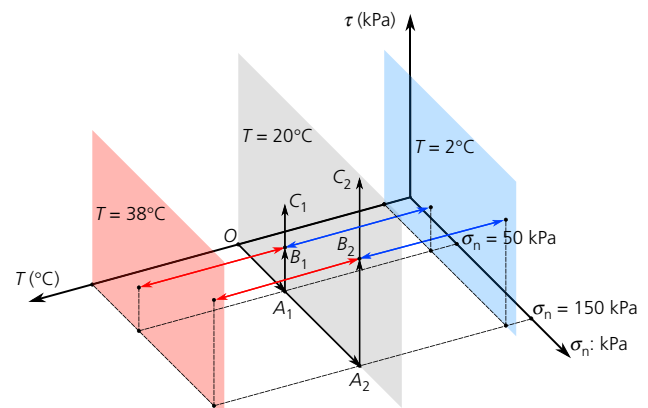
EXPERIMENTAL PROGRAMME

A set of tests was designed to resemble the thermomechanical loading paths of thermo-active geo-structures already subjected to shear stresses, as indicated by the loading paths

presented in Fig. 2. Samples at ambient temperature (20°C) were first consolidated to the desired normal stresses (50 and 150 kPa, corresponding to paths O–A_1 and O–A_2, respectively). With the normal stresses held constant, the samples were then sheared using stress-controlled loading to half of the shear strength (τ_f) on the soil–concrete interface – that is, the ratio of mobilised shear stress (τ) to shear strength (τ/τ_f) reached 0.5 (paths A_1–B_1 and A_2–B_2, respectively, for tests at $\sigma_n = 50$ kPa and $\sigma_n = 150$ kPa). The shear strength values had been obtained by monotonic shearing (at the desired normal stress). Clay– and sand–concrete interfaces were sheared at rates of 0.12 mm/min and 0.25 mm/min, respectively. Samples were then left for 3 h (on average) to allow creep behaviour to evolve. Then, starting from room temperature (20°C), with the shear stress kept constant, samples were subjected to five heating cycles (20–38–20°C) or five cooling cycles (20–2–20°C). Clay– and sand–concrete interfaces were subjected to temperature changes at 3 and 9°C/h, respectively. Finally, at ambient (room) temperature, the samples were sheared to failure under CNL stress conditions (paths B_1–C_1 and B_2–C_2).

RESULTS AND DISCUSSION

The evolution of total shear displacements recorded for the clay– and sand–concrete interfaces when subjected to thermal cycles (with an initially applied shear stress which is kept constant) are shown in Figs. 3 and 4, respectively. It is observed that, for both types of soil, the displacement increased with time. Before being subjected to thermal cycles, the temperature of the samples was kept at 20°C for approximately 2 h. The solid vertical line (shown in green) in Figs. 3 and 4 indicates when the thermal cycles began. Before starting the thermal cycles, the measured displacement of all samples exhibited an almost logarithmic correlation with

Fig. 2. Thermomechanical stress path of the experimental programme; heating cycles and cooling cycles are shown, respectively, by red and blue arrows
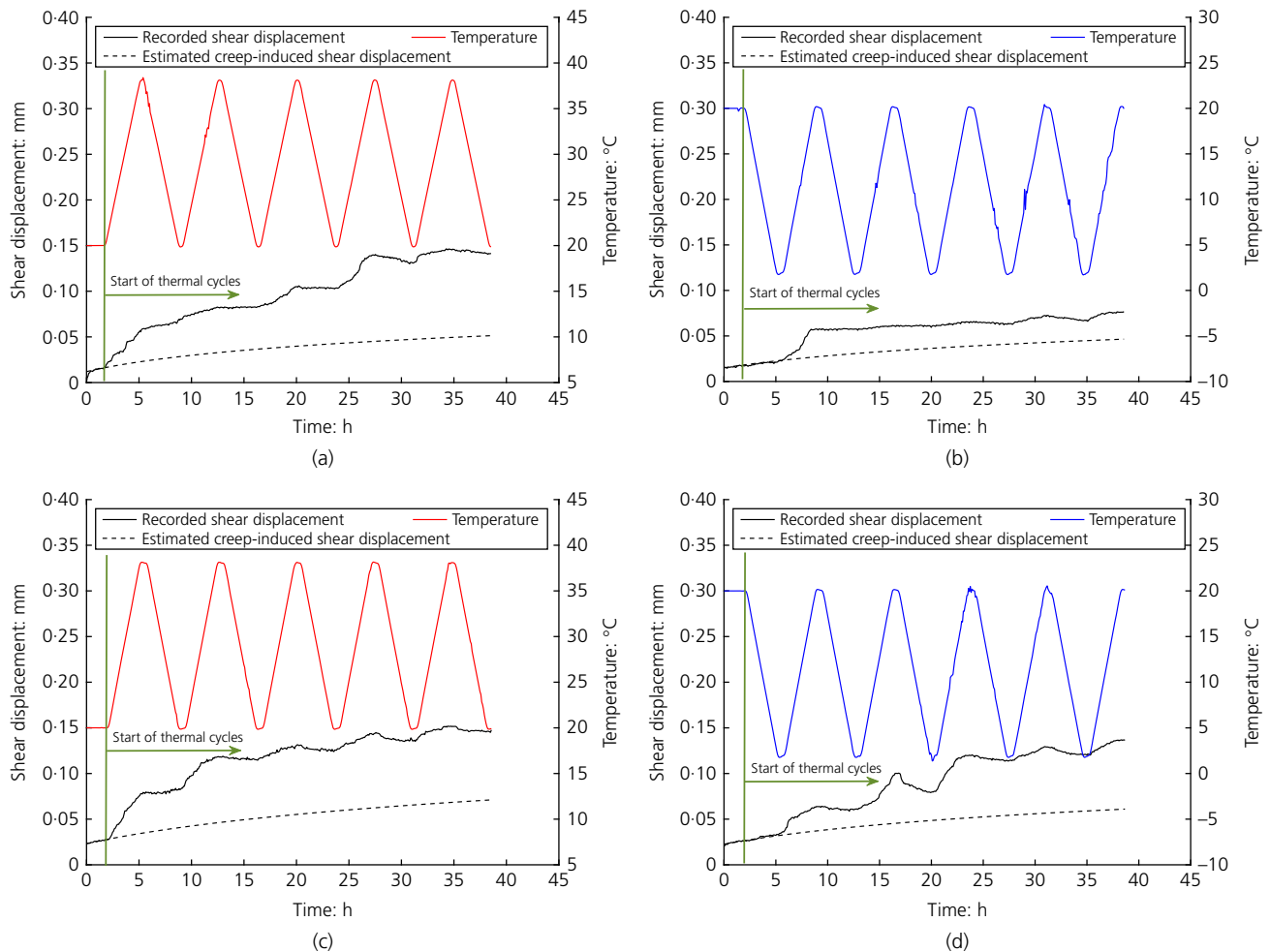
Fig. 3. Evolution of shear displacement of clay–concrete interface during thermal cycles: (a) heating cycles at $\sigma_n = 50$ kPa; (b) cooling cycles at $\sigma_n = 50$ kPa; (c) heating cycles at $\sigma_n = 150$ kPa; (d) cooling cycles at $\sigma_n = 150$ kPa

time (i.e. the measured displacement between time = 0 and the solid line). The shear displacement induced by creep (i.e. with respect to time) was then extrapolated by extending a logarithmic curve fitted to the initial phase of the shear displacement against time curve.

Table 1 presents the measured shear displacements at different stages of the thermomechanical loading paths, including at $\tau/\tau_f = 0.5$, and at the beginning and end of the thermal cycles. Note that shear displacements due to creep are also included in Table 1. The percentage ratio (R_a) of the measured shear displacement during the thermal cycles (ΔL_{TC}) over the measured shear displacement at $\tau/\tau_f = 0.5$ (L_S) for the clay– and sand–concrete interfaces were higher at $\sigma_n = 50$ kPa compared to $\sigma_n = 150$ kPa. For clay–concrete interfaces, R_a varied approximately between 30 and 33% at $\sigma_n = 50$ kPa, and between 21 and 25% at $\sigma_n = 150$ kPa. For sand–concrete interfaces, the corresponding values were lower, with R_a varying approximately between 17 and 19% at $\sigma_n = 50$ kPa, and between 13 and 16% at $\sigma_n = 150$ kPa.

The net shear displacement evolution due to thermal effects was then calculated as the difference between the recorded shear displacement and the estimated shear displacement due to creep. Figure 5 shows the percentage ratio (R_{na}) of the net accumulated temperature-induced shear displacement over the corresponding L_S with respect to the number of thermal cycles. The results show that additional shear displacement (approximately between 13 and 22% of the shear displacement at $\tau/\tau_f = 0.5$ for clay–concrete interfaces and approximately between 6 and 11% of

the shear displacement at $\tau/\tau_f = 0.5$ for sand–concrete interfaces) took place at both the clay– and sand–concrete interfaces as a consequence of temperature variation occurring with a constant shear stress, with most additional shear displacement occurring within the first two thermal cycles. Note that, for most samples, the net shear displacement due to temperature variation increased during heating, whereas it became steadier (or slightly reduced) when the temperature decreased.

After the thermal cycles were completed, the specimens were further sheared until failure. The shear stress against shear displacement curves for the entire process (paths A_1–C_1 and A_2–C_2) for clay– and sand–concrete interfaces, respectively, are presented in Figs. 6 and 7, and are compared with monotonic soil–interface shearing results at ambient temperature in order to identify the changes of ultimate shear strength due to thermal cycles. It is observed that the effect of coupling between thermal cycles and shear stress on the peak and critical state shear strengths, for both types of soil interfaces, was negligible.

The specimens after thermal cycles initially behaved more stiffly (zones A and B in Figs. 6 and 7), with the tangent to the shear stress against shear displacement curves being higher after thermal cycles compared to the corresponding slope before thermal cycles. Such reinforcement was destroyed after a further slight shearing (shear displacements less than 0·1 mm for both types of soil interface) and the stiffnesses returned to a similar level to those of specimens monotonically sheared at ambient temperature.
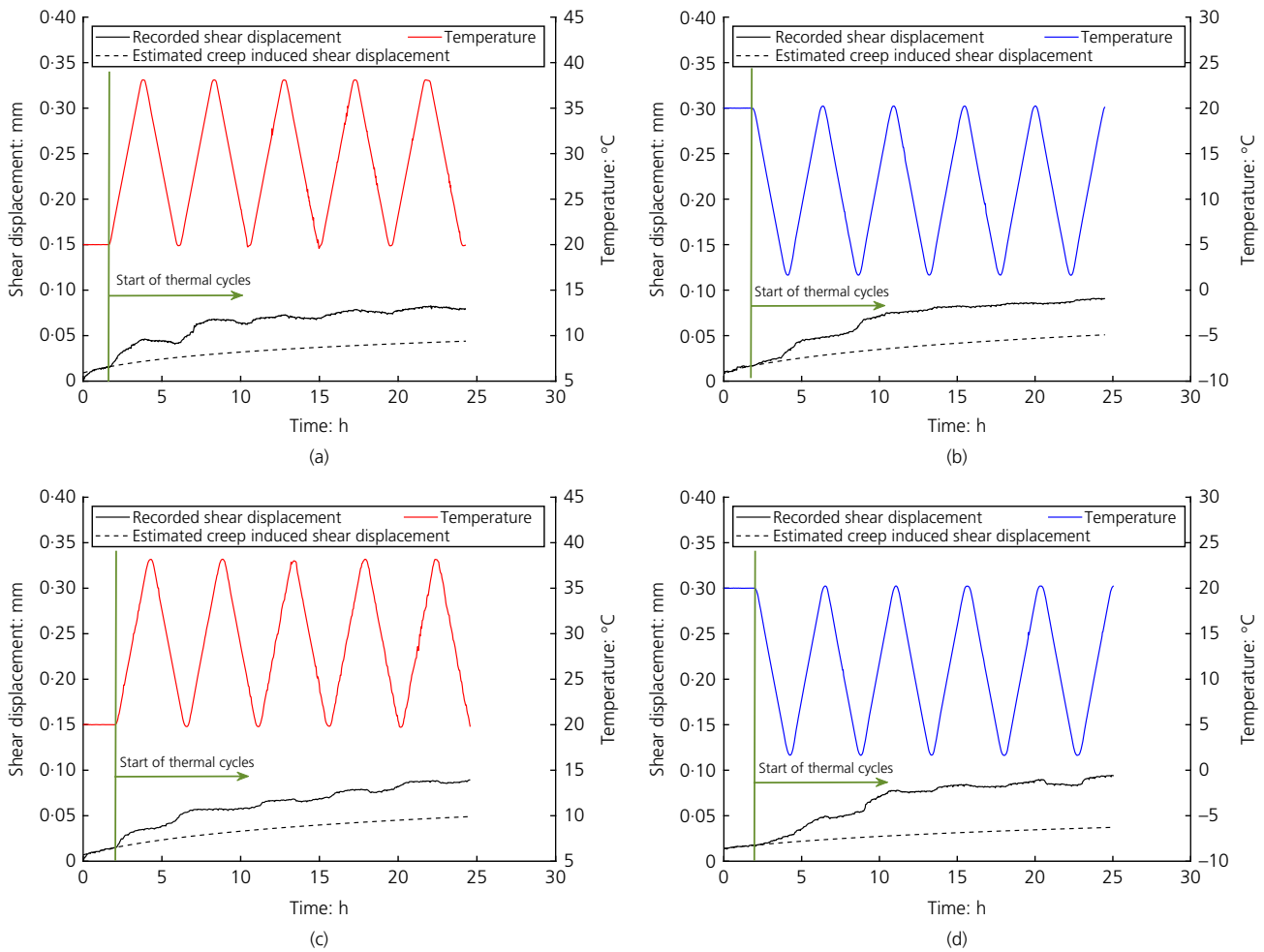
Fig. 4. Evolution of shear displacement of sand–concrete interface during thermal cycles: (a) heating cycles at $\sigma_n = 50$ kPa; (b) cooling cycles at $\sigma_n = 50$ kPa; (c) heating cycles at $\sigma_n = 150$ kPa; (d) cooling cycles at $\sigma_n = 150$ kPa

Table 1. Shear displacement at different stages of thermomechanical loading paths

	Normal stress, σ_n: kPa	Thermal cycles	L_S: mm	L_{TC_ini}: mm	L_{TC_end}: mm	ΔL_{TC}: mm	R_a: %
Clay–concrete interface	50	Heating	0·40	0·42	0·55	0·13	32·5
	50	Cooling	0·20	0·24	0·30	0·06	30
	150	Heating	0·58	0·64	0·76	0·12	20·7
	150	Cooling	0·44	0·48	0·59	0·11	25
Sand–concrete interface	50	Heating	0·37	0·38	0·45	0·07	19
	50	Cooling	0·41	0·46	0·53	0·07	17
	150	Heating	0·63	0·64	0·72	0·08	12·7
	150	Cooling	0·50	0·51	0·59	0·08	16

L_S: shear displacement at $\tau/\tau_f = 0.5$.
L_{TC_ini}: shear displacement at the beginning of thermal cycles.
L_{TC_end}: shear displacement at the end of thermal cycles.
ΔL_{TC}: shear displacement during thermal cycles ($= L_{TC\_end} - L_{TC\_ini}$).
R_a: percentage of the measured shear displacement during thermal cycles with respect to the measured shear displacement at $\tau/\tau_f = 0.5$ ($= \Delta L_{TC}/L_S \times 100$).

For the first time, the phenomenon of shear displacements of soil–concrete interfaces under thermal cycles, where the interface is subjected to a constant shear stress, has been observed. The process is complex and may be explained by utilising and combining several aspects of existing knowledge on the thermomechanical mechanism of sands and clays, the micro- and macro-mechanical interaction between soil grains, and energy generation and dissipation (energy level changes) at the interface level (thermodynamics perspective).

The 'interface layer' between soils and structures (in this study, a soil–concrete interface) is a thin layer of the soil that is in contact with the structure. Therefore, the thermomechanical behaviour of soils may (partially) govern the thermomechanical behaviour of the interface layer.

The thermomechanical behaviour of saturated sandy soils is mostly dominated by the difference in the volumetric thermal expansion coefficients between the soil particles and water, as well as the change in the viscosity of water due to
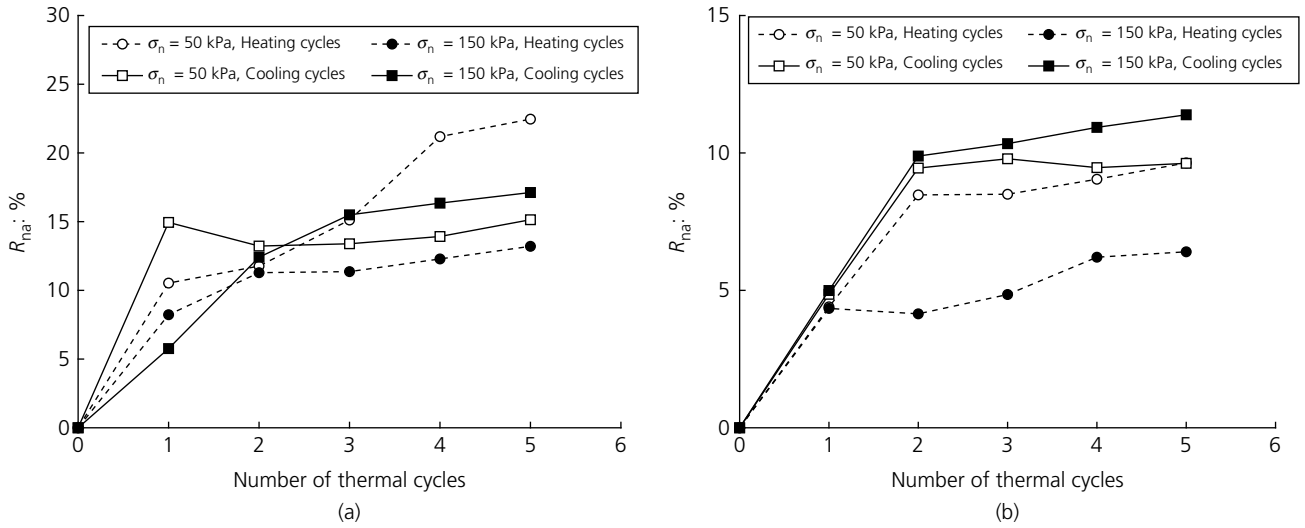
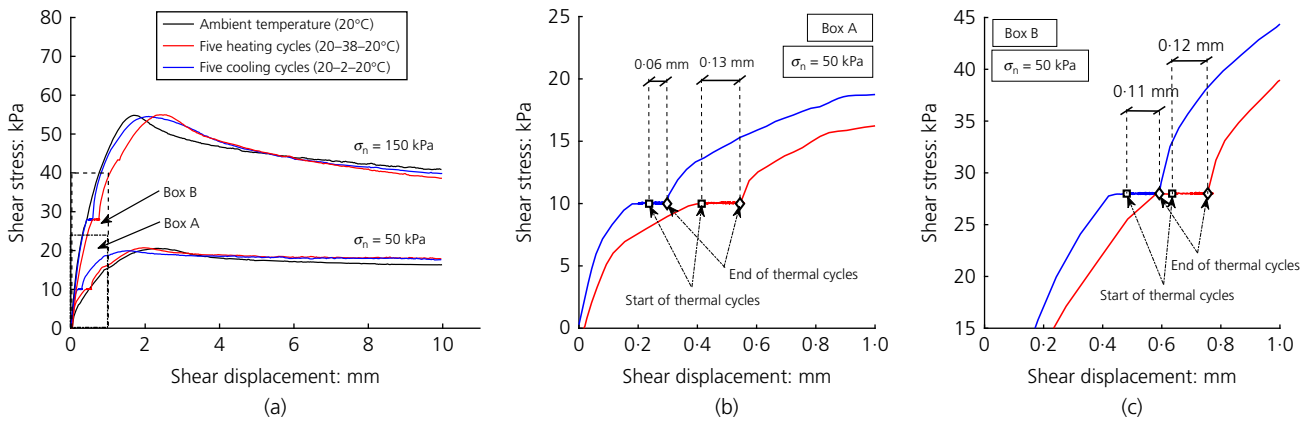**Fig. 5.** R_{na}: (a) clay–concrete interfaces; (b) sand–concrete interfaces

Fig. 6. Shear stress against shear displacement of clay–concrete interface: (a) all specimens; (b) magnified box A for the samples at $\sigma_n = 50$ kPa; (c) magnified box B for the samples at $\sigma_n = 150$ kPa

Fig. 7. Shear stress against shear displacement of sand–concrete interface: (a) all specimens; (b) magnified box A for the samples at $\sigma_n = 50$ kPa; (c) magnified box B for the samples at $\sigma_n = 150$ kPa
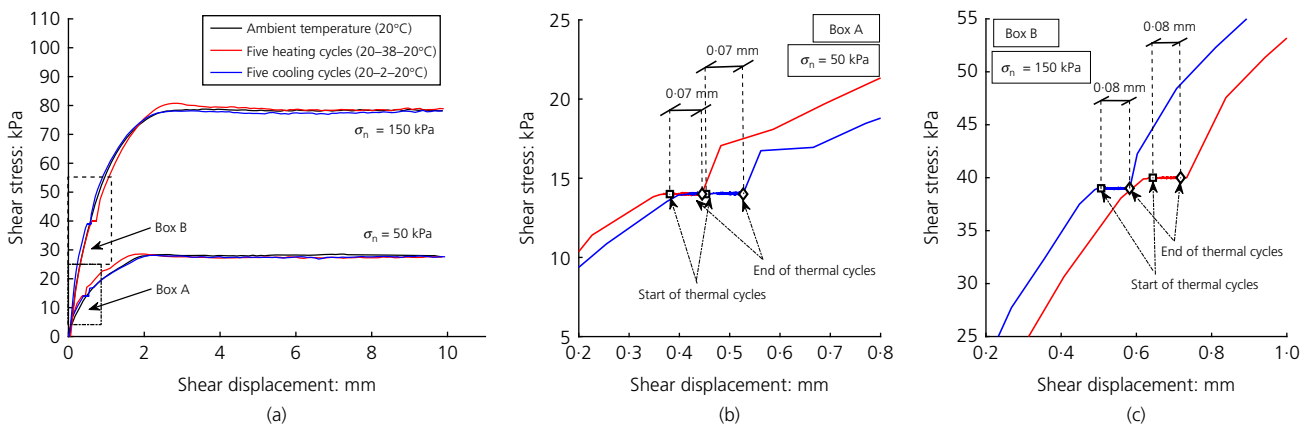
temperature variation (Russell Coccia & McCartney, 2012; Vega & McCartney, 2015).

On the contrary, the thermomechanical behaviour of saturated fine-grained soils, especially clayey soils, is dominated by physicochemical internal forces which result in changes in the thickness of the hydration layers of soil particles, and the development of '*disjoining pressures*' (see Golchin *et al.* (2022) for more details). In addition, Houhou

et al. (2021) demonstrated that thermal loads affect the microstructure of clayey soils, which are formed by clay particles and pores between them (pores varying in size; i.e. micro- and macro-size, and the pore-density). Due to thermal loads, macro-size pores may collapse and/or the soil may experience a change in the pore-density, while micro-size pores are less affected or remain intact (Houhou *et al.*, 2021). In both of these cases (sands and clays), the cyclic thermal loads impact the force chains on a micro-scale allowing additional shear deformation to occur under constant shear stress when subjected to thermal cycles.

In addition, the micro- and macro-mechanics at the interface level significantly affect the mechanical response of the interface layer. The initial shear loading induces shear forces/stresses between the soil particles. The normalised roughness between the soil and the structure also influences the level of mobilised forces/stresses; larger values of normalised roughness result in higher mobilised forces/stresses at the interface layer and potentially failure through the soil, not at the interface. In this study, an intermediate roughness of the interface is found, which implies that failure at the interface and in the soil at the same time is likely to occur (Guo *et al.*, 2023). In such a case, the representative volume element (RVE) of the material in contact with the structure (at the interface level) may be considered to be comprised of two fractions associated with strong and weak force chains (Collins, 2005), where the majority of the shear deformations (plastic deformations) occur in the fraction of the RVE corresponding to weak force chains as a result of inter-grain slippage and rotation (Radjai *et al.*, 1996, 1998).

When the temperature changes at the interface level, due to governing thermomechanical mechanisms (e.g. development of disjoining pressures for clayey soils and thermal expansion of particles and water for sandy soils), the macro-size pores in the fraction of the material associated with weak force chains may collapse. Consequently, the thermodynamically stable state of the soil can be prone to a thermodynamically unstable state. At the thermodynamically unstable state caused by heating, soil particles rotate and reorientate temporarily (mostly in the fraction associated with weak force chains), which results in the observed evolution of shear displacement. This process continues until soil particles attain a sufficient number of contacts with adjacent particles and sufficient interlocking stresses are mobilised. Consequently, a new thermodynamically stable state is reached. The increase in the interlocking stresses, and in the area and number of contacts between particles, forms a new micro- and macro-mechanical structure inside the soil with macro-size pores reduced in size compared to before thermal loading. After several thermal cycles, the sizes of the macro-size pores are sufficiently reduced so that the pores may not be affected by thermal loads, leading to a cessation in shear displacement development which is consistent with the observed experimental results. This mechanism may be the main reason for the observed stiffer behaviour of the shearing after thermal cycles were applied to the soil (Figs. 6 and 7).

CONCLUSION

To investigate the thermomechanical stress and temperature histories that soils experience at the interface level of thermo-active geo-structures such as energy piles, a set of experiments was conducted to investigate the coupling effect of shear stress and thermal cycles on the behaviour of soil–concrete interfaces. Samples were sheared to half of the interface's shear strength prior to being subjected to five heating/cooling cycles. The results indicated that shear displacements evolved when soil–concrete interfaces were subjected to thermal cycles, although only negligible changes in shear strength were observed. This is an important observation which should be considered in the design procedure of thermo-active structures. The observed temperature-induced shear displacements under constant shear stresses may result in additional and unwanted settlements during the serviceability life-time of these structures, especially for those whose main load-transfer mechanism to the soil and bearing capacity are through skin-friction mobilisation such as floating piles. Although a slight increase of stiffness was observed after thermal cycles under constant shear stresses, due to the newly formed micro- and macro-mechanical structures in the soil, these structures appear to be destroyed by subsequent shearing due to additional loading.

REFERENCES
Boulon, M. & Foray, P. (1986). Physical and numerical simulation of lateral shaft friction along offshore piles in sand. In *3rd international conference on numerical methods in offshore piling*. pp. 127–147. Nantes, Paris: Editions Technip.
Brandl, H. (2006). Energy foundations and other thermo-active ground structures. *Géotechnique* **56**, No. 2, 81–122, https://doi.org/10.1680/geot.2006.56.2.81.
Collins, I. F. (2005). Elastic/plastic models for soils and sands. *Int. J. Mech. Sci.* **47**, No. 4–5, 493–508.
Di Donna, A., Ferrari, A. & Laloui, L. (2016). Experimental investigations of the soil–concrete interface: physical mechanisms, cyclic mobilization, and behaviour at different temperatures. *Can. Geotech. J.* **53**, No. 4, 659–672.
Fakharian, K. & Evgin, E. (1997). Cyclic simple-shear behavior of sand-steel interfaces under constant normal stiffness condition. *J. Geotech. Geoenviron. Engng* **123**, No. 12, 1096–1105.
Golchin, A., Vardon, P. J. & Hicks, M. A. (2022). A thermomechanical constitutive model for fine-grained soils based on thermodynamics. *Int. J. Engng Sci.* **174**, 103579.
Guo, Y., Golchin, A., Hicks, M. A., Liu, S., Zhang, G. & Vardon, P. J. (2023). Experimental investigation of soil–structure interface behaviour under monotonic and cyclic thermal loading. *Acta Geotech*, https://doi.org/10.1007/s11440-022-01781-5.
Houhou, R., Sutman, M., Sadek, S. & Laloui, L. (2021). Microstructure observations in compacted clays subjected to thermal loading. *Engng Geol.* **287**, 105928.
Li, C., Kong, G., Liu, H. & Abuel-Naga, H. (2019). Effect of temperature on behaviour of red clay–structure interface. *Can. Geotech. J.* **56**, No. 1, 126–134.
Maghsoodi, S., Cuisinier, O. & Masrouri, F. (2020). Thermal effects on mechanical behaviour of soil–structure interface. *Can. Geotech. J.* **57**, No. 1, 32–47.
Makasis, N. & Narsilio, G. A. (2020). Energy diaphragm wall thermal design: the effects of pipe configuration and spacing. *Renew. Energy* **154**, 476–487.
Radjai, F., Jean, M., Moreau, J. J. & Roux, S. (1996). Force distributions in dense two-dimensional granular systems. *Phys. Rev. Lett.* **77**, No. 2, 274–277.

Radjai, F., Wolf, D. E., Jean, M. & Moreau, J. J. (1998). Bimodal character of stress transmission in granular packings. *Phys. Rev. Lett.* **80**, No. 1, 61–64.

Ravera, E., Sutman, M. & Laloui, L. (2021). Cyclic thermomechanical response of fine-grained soil–concrete interface for energy piles applications. *Can. Geotech. J.* **58**, No. 8, 1216–1230.

Russell Coccia, C. J. & McCartney, J. S. (2012). A thermo-hydro-mechanical true triaxial cell for evaluation of the impact of anisotropy on thermally induced volume changes in soils. *Geotech. Test. J.* **35**, No. 2, 103803.

Vasilescu, R., Yin, K., Fauchille, A. L., Kotronis, P., Dano, C., Manirakiza, R. & Gotteland, P. (2019). Influence of thermal cycles on the deformation of soil-pile interface in energy piles. In *Proceedings of the 7th international symposium on deformation characteristics of geomaterials* (eds A. Tarantino and E. Ibraim), vol. 92, paper no. 13004. Les Ulis, France: E3S Web of Conferences.

Vega, A. & McCartney, J. S. (2015). Cyclic heating effects on thermal volume change of silt. *Environ. Geotech.* **2**, No. 5, 257–268.

Yavari, N., Tang, A. M., Pereira, J. M. & Hassen, G. (2016). Effect of temperature on the shear strength of soils and the soil–structure interface. *Can. Geotech. J.* **53**, No. 7, 1186–1194.

Yazdani, S., Helwany, S. & Olgun, G. (2019). Influence of temperature on soil–pile interface shear strength. *Geomech. Energy Environ.* **18**, 69–78.

HOW CAN YOU CONTRIBUTE?

To discuss this paper, please submit up to 500 words to the editor at journals@ice.org.uk. Your contribution will be forwarded to the author(s) for a reply and, if considered appropriate by the editorial board, it will be published as a discussion in a future issue of the journal.